Video Article

Visualization of Endosome Dynamics in Living Nerve Terminals with Four-dimensional Fluorescence Imaging

Richard S. Stewart[1], Ilona M. Kiss[1], Robert S. Wilkinson[1]

[1]Department of Cell Biology and Physiology, Washington University School of Medicine

Correspondence to: Robert S. Wilkinson at WILK@wustl.edu

URL: https://www.jove.com/video/51477
DOI: doi:10.3791/51477

Keywords: Neuroscience, Issue 86, Microscopy, Fluorescence, Endocytosis, nerve, endosome, lysosome, deconvolution, 3D, 4D, epifluorescence

Date Published: 4/16/2014

Citation: Stewart, R.S., Kiss, I.M., Wilkinson, R.S. Visualization of Endosome Dynamics in Living Nerve Terminals with Four-dimensional Fluorescence Imaging. *J. Vis. Exp.* (86), e51477, doi:10.3791/51477 (2014).

Abstract

Four-dimensional (4D) light imaging has been used to study behavior of small structures within motor nerve terminals of the thin transversus abdominis muscle of the garter snake. Raw data comprises time-lapse sequences of 3D z-stacks. Each stack contains 4-20 images acquired with epifluorescence optics at focal planes separated by 400-1,500 nm. Steps in the acquisition of image stacks, such as adjustment of focus, switching of excitation wavelengths, and operation of the digital camera, are automated as much as possible to maximize image rate and minimize tissue damage from light exposure. After acquisition, a set of image stacks is deconvolved to improve spatial resolution, converted to the desired 3D format, and used to create a 4D "movie" that is suitable for variety of computer-based analyses, depending upon the experimental data sought. One application is study of the dynamic behavior of two classes of endosomes found in nerve terminals-macroendosomes (MEs) and acidic endosomes (AEs)-whose sizes (200-800 nm for both types) are at or near the diffraction limit. Access to 3D information at each time point provides several advantages over conventional time-lapse imaging. In particular, size and velocity of movement of structures can be quantified over time without loss of sharp focus. Examples of data from 4D imaging reveal that MEs approach the plasma membrane and disappear, suggesting that they are exocytosed rather than simply moving vertically away from a single plane of focus. Also revealed is putative fusion of MEs and AEs, by visualization of overlap between the two dye-containing structures as viewed in each three orthogonal projections.

Video Link

The video component of this article can be found at https://www.jove.com/video/51477/

Introduction

Time-lapse imaging of living tissue provides visual access to dynamical structure-function relations that cannot be appreciated in fixed or living preparations imaged at a single point in time. Often, however, the tradeoff for access to temporal information is a decrease in optical resolution. High numerical aperture oil-immersion objectives are impractical in living tissue because of their narrow range of focus, leaving water immersion or dry objectives as the only alternatives. Moreover, the increased resolution afforded by confocal optics cannot be utilized in some living preparations due to phototoxicity from the relatively high levels of illumination required[1,2]. Lastly, while several real-time or time-lapse optical techniques are available that offer enhanced resolution, their applicability is limited to preparations where structures of interest can be positioned within a few hundred nanometers of the objective[1]. The method described makes use of relatively low-cost equipment, is versatile, yet offers improved resolution compared to more commonly-used time-lapse techniques. It is intended for use in individual laboratories as well as imaging facilities.

The method utilizes conventional epifluorescence microscopy, combined with a sensitive digital camera and with hardware designed to rapidly acquire sets of images at slightly different focal planes (z-stacks). Each z-stack is digitally deconvolved to increase resolution. One feature of 3D time-lapse (4D) imaging is precise tracking of moving organelles or other structures. When properly set up, imaged structures do not go out of focus, and movement in all three directions can be observed and quantified. Thus it is impossible for a stained structure to disappear over one or more time-lapse frames merely by drifting above or below a narrow focal plane. The method also serves as a sensitive tool for assessing the interactions and possible fusion of small structures. Conventional epifluorescence or confocal images of structures near the diffraction limit (a few hundred nm) do not confirm fusion even if merged images show overlap of their respective labels[3]. Fusion is suggested, but it remains possible that the objects are separated horizontally or vertically by a distance that is below the diffraction limit. Three- or four-dimensional imaging, in contrast, permits viewing the objects in each of three orthogonal directions. The appearance of fusion in all three views increases the level of certainty. And, in some living preparations, directed or Brownian movement of putatively fused objects provides further proof when both labels move together in time. Of course, when near the diffraction limit the level of certainty in discerning structures from background, or showing that they contain two dyes (fusion), is not absolute. If applicable, specialized techniques, such as fluorescence resonance energy transfer (FRET)[4], are more appropriate.

Protocol

1. Stain the Preparation with Supravital Dyes

1. For the garter snake dissection protocol see Stewart *et al.*[5] and Teng *et al.*[6] Reptilian tissue remains physiological for longer times, and with less bacterial contamination, when kept at low temperatures (see below). Mammalian tissue is usually maintained at room temperature or higher.
2. For lysosomal vital dye staining, dissolve the dye in cold reptilian Ringers solution 1:5,000 (0.2 µM). Incubate at 4 °C for 15 min. Wash several times with cold Ringers. Image as soon as possible.
3. For FM1-43 staining using KCl stimulation, dilute the dye in high-KCl Ringers 1:500 (7 µM). Incubate at 4 °C for 30-60 sec maximum. Wash quickly three times with cold Ringers, ~1 min/rinse. Image as soon as possible.
4. For FM1-43 staining using hypertonic (sucrose) stimulation, dilute the dye in 0.5 M sucrose Ringers as above. Incubate at 4 °C for 2-5 min. Wash as in step 1.3 above with cold Ringers. Image as soon as possible.
5. For FM1-43 staining via electrical stimulation, see Teng *et al.*[6] Briefly, the preparation is placed a dish containing physiological saline solution and the dye. The nerve is stimulated with a preprogrammed train of 200 µsec rectangular pulses (~7 V, 30 Hz, 18 µsec). Wash as in step 1.3 above with cold Ringers. Image as soon as possible.

2. Configure the Preparation for Imaging

1. Orient the preparation so that structures of interest are as close as possible to the microscope objective.
2. If an inverted microscope is used, utilize a chamber whose bottom contains a thin round cover slip. Typically, the imaging chamber should have a thin stainless steel bottom with a 25 mm diameter #1 thickness glass cover slip at the center. If an upright microscope is used, a bottom coverslip is not required but is useful to permit imaging with transmitted light (*e.g.* differential interference contrast, DIC) to orient the specimen and locate objects of interest.
3. Choose an appropriate objective to obtain the highest possible 3D resolution. There are tradeoffs among numerical aperture (n.a.), working distance, magnification, and type of lens (dry, water- and oil-immersion). For thin preparations like tissue cultures, oil objectives are best. Using an upright microscope, float a cover slip on the aqueous bath, and use immersion oil between the top of the cover slip and the objective.
4. If deconvolution software is used, the vendor might provide predetermined point spread functions (PSFs) for certain objectives. If no such information is provided, or if an unsupported objective is chosen, determine the PSF by imaging fluorescent microdots or similar diffraction-limited objects[7,8].

3. Establish the Desired Depth of Field and Number of Images Desired per Time-lapse Frame

1. Select the total depth of field so that moving or interacting structures of interest do not disappear or go out of focus as they move in the z-direction. The z-field should slightly exceed the vertical dimension of the cell or cell process being imaged. For vertebrate motor terminals, 15-20 µm is typical.
2. Calculate the z-axis step needed for each increment of focus. Resolution along the z-axis varies depending upon properties of the objective; it is about one-fourth of the x-y plane resolution. If either confocal imaging or deconvolution software is used, z-axis resolution is improved. Improve final resolution by deliberate oversampling in the z-direction [5], but see also step 3.3 below. A typical step interval is in the range from 400-1,500 nm for 40-100X objectives. Light should be shuttered off between each z-step image.
3. Select the number of images per z-stack, namely the desired depth of field divided by the step interval. Time to complete a typical z-stack is 1-10 sec. Fast-moving objects (100 nm/sec) can appear blurred in a 3D image stack because each image plane corresponds to a slightly different time point. Also, each additional image contributes to photobleaching and possible phototoxicity (see Discussion). If either situation pertains, choose a larger z-step to collect fewer images per stack. Compensate later using image interpolation software (step 6.3 below).

4. Select the Time-lapse Frame Rate

Choose by experimentation a rate that is just adequate to smoothly resolve changes with time such as movement, interactions or fusion events[9]. Under sampling can produce motion artifacts (sampling errors), while oversampling unnecessarily increases exposure to light. Collect either a single long sequence or several repeated sequences from the same preparation, each with a relatively small total time interval (*e.g.* 10 time points x 30 sec interval = 5 min). If possible, view the preparation with continuous epifluorescence illumination to roughly estimate movement velocities, including drift of the entire preparation if present.

5. Complete All Live Imaging for a Particular Preparation

Reptilian preparations typically remain robust for ~1-2 hr, longer if cooled.

6. Analyze Data According to Desired Use

1. Retain all raw data files. While digital storage is usually not a problem, processing time is significant even with fast personal computers or workstations. For this reason, crop images into a region of interest [ROI]. Assure that the entire region of interest is in the cropped window during the entire time course.

2. Deconvolve image stacks using appropriate software and the correct point spread function. Confirm that resolution is improved and that no artifact has been generated by the deconvolution algorithm. **Figure 3** shows example images.
3. Use an interpolation algorithm to expand z-axis apparent resolution. A 6X expansion from an actual 1.5 µm image plane separation to an apparent 0.25 µm separation is suggested. Alternatively, use some combination of oversampling (step 3.2) and interpolation.
4. Perform contrast, brightness, noise filtering, photobleaching and other typical image processing adjustments if desired. Image manipulation standards dictate that for most scientific work, it is appropriate that the same corrections be applied to all images, both within a stack and at different time points. The consequence of a particular adjustment should be assessed among all images [9].
5. Select a particular display mode for export of data. The most straightforward display is stereo video using either red-green or red-blue anaglyphs (examples in **Figure 3**), stereo pairs, or alternating left/right eye frames with shutter glasses. Anaglyphs are limited to single-color. Enhance apparent image depth if desired to improve z-axis visual resolution.
6. Experiment with various filtering and image enhancement techniques. For example, Laplacian filtering is useful to increase contrast of small structures above background. The brightness of pixels at the center of a running window is enhanced while brightness of surrounding areas is reduced. Note that some filtering methods do not work well in combination.
7. Apply drift correction if there is substantial movement of the preparation over time. Such movement is common in living muscle, even with drugs added to suppress action potentials and synaptic potentials. A pixel registration algorithm (*e.g.* IMARIS, Adobe AfterEffects, TurboReg plugin for ImageJ) aligns time-lapse images and can reduce, but usually not completely eliminate, such motion.

Representative Results

Data shown are from snake neuromuscular terminals (see low and high magnification views in **Figure 3**; the endocytic dye (FM1-43) uptake creates a haze that fills each bouton) and, in particular, macroendosomes (MEs) and acidic endosomes (AEs) within these terminals[5]. MEs are created by bulk endocytosis during neural activity[10] and their number declines exponentially with time after activity has ceased[6]. Use of 4D live imaging was to determine if MEs move towards the plasma membrane and quickly disappear, suggesting that their number decreases because some of them exocytose. All such MEs were present at one time point (and those before) and completely gone at the next time point (and those after). Thus the time required for disappearance was less than our frame interval (as short as 30 sec) and consistent with exocytosis. An alternative theory, not supported by 4D data, is that MEs slowly dissipate via budding of vesicles until they vanish. Vesicle budding occurs[6], but at least some MEs are exocytosed either during or after budding[5]. **Figure 1** and **Movie S1** illustrate the disappearance of a ME between two time-lapse frames. MEs destined to vanish did not change shape or brightness over two or more frames (N = 16), which would have been consistent with slow dissipation during the time period of the movie (beginning several min after brief stimulation). ME disappearance was observed previously in conventional time-lapse, but it was possible that the structures had simply left the plane of focus. Moreover, viewing from a variety of perspectives (**Movie S1**) confirmed that the ME disappearance was sudden. With conventional live imaging (looking from a single perspective, *e.g.* the x-y image plane) noise artifacts limit the investigator's ability to confirm that a structure was unchanged. Such artifacts are often present in one view but not others.

Electron microscopy studies showed that endosomes in motor terminals are small in size, near the diffraction limit of light[10]. Hence fusion of these endosomes cannot be absolutely distinguished from close spatial association at light level. MEs were labeled with FM1-43 (green-fluorescing), and AEs with a lysosomal vital dye (red-fluorescing). Structures that fluoresced in both colors (appearing yellow) were occasionally noted in 4D image records. Using appropriate software, views of these double-labeled and therefore apparently fused endosomes from a variety of perspective were generated in order to examine the coincidence of the two labels in voxels near and within the apparent structure. **Figure 2** shows a putative fused AE-ME as viewed from three orthogonal directions. One view is the x-y plane; the other views are orthogonal to that plane and to each other. Using this method it was found that voxels either overlapped, as in this example, or that they clearly didn't in one or more viewing planes. **Movie S2** shows the same putative fused AE-ME presented as an interactive virtual reality display (fully rotatable in 3 dimensions).

Digital deconvolution is a useful tool to enhance resolution of 3D as well as 4D images, from both conventional and confocal microscopes[11]. Deconvolution is a numerical, iterative process that compensates, to some extent, for limited spatial resolution of the objective used. This resolution is characterized as the objective's point spread function—the 3D volume occupied by the image of an infinitesimal point. In theory, deconvolution restores the image that would result if the objective were perfect. **Figure 3** is a 3D volume view of two different data sets, each displayed as a pair of red-green anaglyphs. The right images show typical improvement in sharpness after digital deconvolution of the image stack.

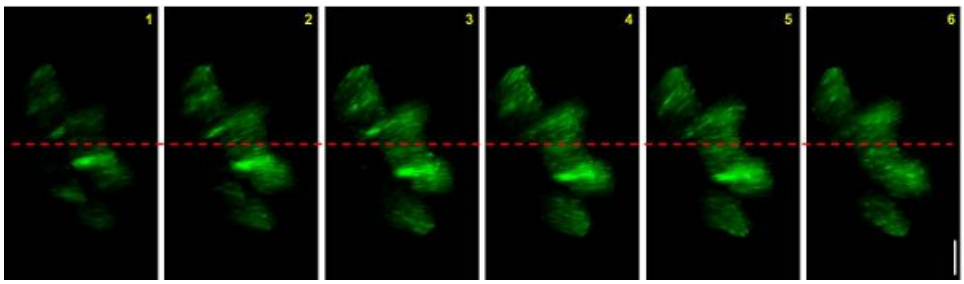

Figure 1. A macroendosome (ME) disappears after apparent contact with plasma membrane. A snake nerve-muscle preparation was electrically stimulated in the presence of FM1-43. Data were collected using 4D imaging as described in Methods and are displayed as "3D Volume views" at six time points (60 sec interval) to illustrate the Z-depth of a single bouton. An ME can be observed moving away from the Y axis (red dashed line) over several frames before disappearing between time points 5 and 6. Just before disappearance, the ME appears to be located at the bouton's plasma membrane (delineated by FM1-43 vesicle staining or "haze;" see **Figure 3** legend). The ME did not reappear in later time-points (data not shown; see **Movie S1**). Scale bar, 2 µm. Please click here to view a larger version of this figure.

MOVIE S1: 4D time-lapse views of ME disappearance. Click here to view movie. The same raw data set displayed in **Figure 1** is shown as a "4D volume view" at a lower magnification. The original time-lapse sequence comprises 8 time-points, each separated by 60 sec; playback is at 4 frames/sec. The sequence is briefly paused at the beginning of each of 24 3D rotation steps about the y-axis (15 degrees/step) to draw attention to the soon-to-be disappearing ME (red arrow). Note that the ME is visible, approaches the edge of the bouton (plasma membrane), disappears, and doesn't return, in all viewing perspectives. Because of lower z-axis resolution compared to x-y resolution, the shape of the ME appears to lengthen and shorten depending on viewing perspective. Images were exported as a QuickTime movie, and annotated using QuickTime Pro. Scale bar, 2 µm.

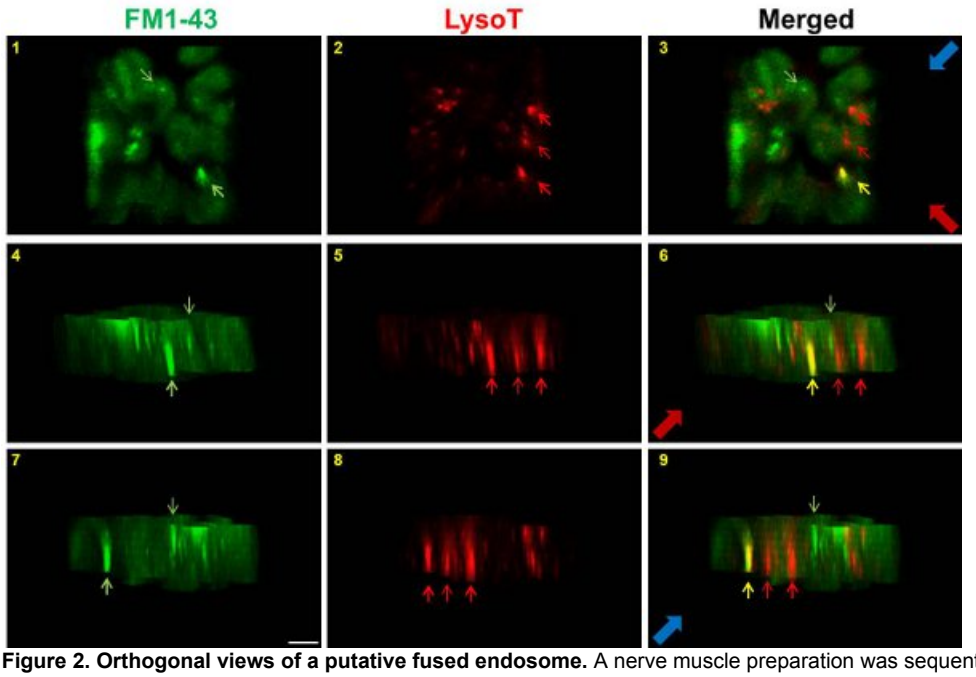

Figure 2. Orthogonal views of a putative fused endosome. A nerve muscle preparation was sequentially stained with a lysosomal vital dye (red) to label AEs and FM1-43 (green) to label MEs using 0.5 M sucrose stimulation as described in Methods. Data from one time point of a 4D movie are displayed as 3D volume views in three orientations. At top (panels 1-3) is the conventional view from above (x-y plane). At middle (panels 4-6) is a view perpendicular to the x-y plane and in the (arbitrary) direction of the large red arrow. At bottom (panels 7-9) is a view mutually perpendicular to both views above, in the direction of the large blue arrow. An ME (green) is marked by a green arrow; two AEs (red) are marked by red arrows. An endosome containing both dyes (yellow) is marked by a yellow arrow in panels 3, 6, and 9. Note that overlap of red and green is equally complete in all three orthogonal projections. Scale bar, 2 µm. Please click here to view a larger version of this figure.

MOVIE S2: Interactive rotation of image containing MEs and acidic endosomes AEs. Click here to view movie. The data set of **Figure 2** is shown configured as a fully rotatable 3D image (QuickTime Virtual Reality format; use the mouse to rotate the image for viewing from any direction). The putative fused ME/AE remains yellow from all perspectives.

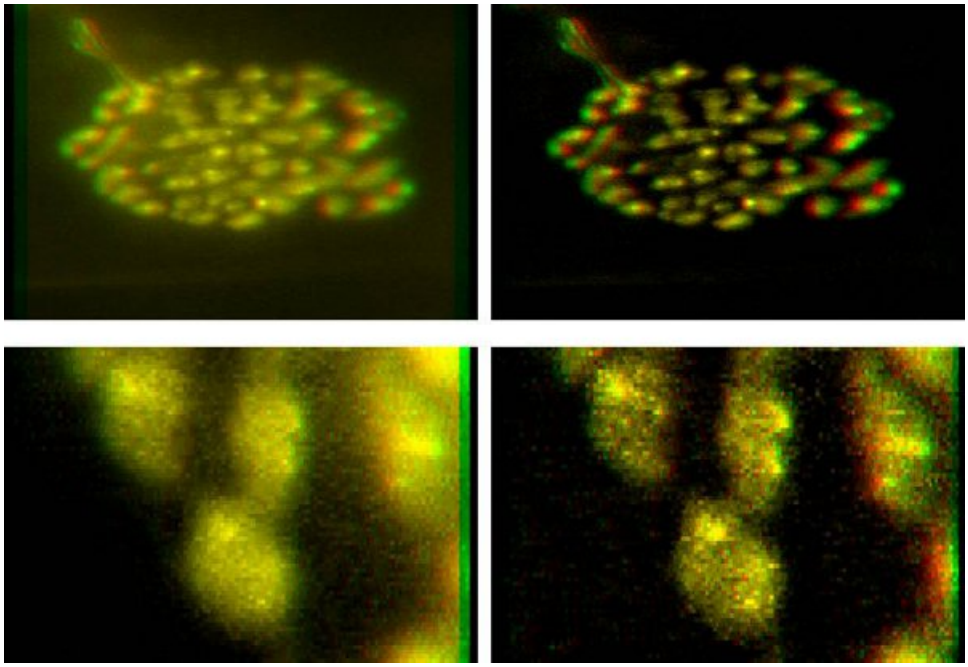

Figure 3. Deconvolution enhances 3D spatial resolution. Two typical snake nerve terminals, shown at low (top) and high (bottom) magnification respectively and stained during stimulation with FM1-43. FM1-43 background "haze," due to labeling of individual 50 nm vesicles, shows the shape of terminal boutons within which MEs are confined. Data are displayed as Red-Green anaglyphs of 3D volume views (depth can be visualized with red-green or red-blue glasses; red on left eye; note axon at upper left descends into the plane of the terminal from above). Left panels: raw data; Right panels: data after deconvolution. Note the significant improvement in resolution of MEs. Top panels: Electrical stimulation; entire terminal shown (~30 x 50 µm) (same raw data as in **Figure 1** and **Movie S1**; scale bar, 10 µm). Bottom panels: KCl stimulation; magnified to show four individual boutons (~3 x 5 µm; scale bar, 2 µm). Please click here to view a larger version of this figure.

Discussion

The most critical aspect of 4D imaging is management of the duration and intensity of light exposure. Photobleaching decreases image signal-to-noise ratio and can be problematic or not depending on various factors, including choice of fluorophores. Nonspecific damage to living tissue (phototoxicity) is related to photobleaching, and can sometimes be identified using fluorescent probes designed for the purpose[2,12] or by examination of morphology with suitable brightfield optics, such as differential interference contrast (DIC).

It is possible, however, to induce a physiological effect that occurs at light levels well below the magnitude of those associated with photobleaching and phototoxicity. For example, in early experiments using multiple preparations, each fixed at a different time after stimulation, the rate at which MEs disappeared with time after a brief stimulation was measured[6]. As is standard practice to minimize fading, preparations were kept in the dark until they were viewed. When similar experiments were performed using 4D live imaging, many more MEs remained throughout the experiment (~20-60 min) and did not disappear. Use of the same live imaging protocol, except not actually recording and thereby limiting light exposure to a single 3D frame at the beginning and a single frame at the end, restored the expected overall rate of endosome disappearance to that of fixed preparations.

Further troubleshooting indicated that the rate of disappearance was in part, inversely and monotonically related to total light exposure during an experiment. After unsuccessful attempts to reduce exposure via conventional and multiphoton confocal optics, the problem was finally resolved by purchase of a ~3x more sensitive camera (**Table 1**). It is recommended that similar comparisons be made if possible, depending on the user's application. If some process or transition is being documented over time, confirm that there is no modification attributable to intensity or total duration of illumination. Phototoxicity and photobleaching are dye-specific. For example, we saw no significant fading after repeated 4D imaging of one terminal (350 individual light exposures over 30 min) using FM1-43. The same imaging protocol using a similar dye, SGC5 (**Table 1**), however, resulted in some fading and, presumably, phototoxicity as well (data not shown).

With the exception of improvements provided by digital deconvolution (and confocal optics if used; not shown), the straightforward method described provides no "super" resolution. However, the method has the advantage of improving practical or intuitive resolution when viewing living structures, particularly moving ones, whose size is at or slightly larger than the diffraction limit. The ability to view objects from various perspectives, including presentation in each of three orthogonal planes, guides the investigator as to whether a structure actually exists above the noise level and whether it is labeled by one or more fluorophores. For example, in experiments designed to quantitate the number and size of MEs and AEs, it was possible to confirm that the structure was visible from various perspectives and that each dimension (and hence its three-dimensional volume) was within the range typical for that structure. The location of a structure is also better defined, for example, within an axon, nerve terminal *etc*. rather than above or below it. In contrast, when the field of view was confined either to a single 2D image plane or to a single projection of 3D data, putative structures often proved to be "noise." Similarly, putative double-labeled structures often proved to be two structures that appeared coincident from one viewing perspective (or two) but not from all. Visualization from three orthogonal directions provides a standard and routine criterion for assessing the existence, size, and labeling characteristics of endosomes or similar structures for use in quantitative and statistical analyses.

The methodology described is practical in that a conventional video microscope of the type found in many laboratories can be used. The instrumentation is versatile rather than specialized, and relatively inexpensive. While software specific to a particular microscope was used here, open-source software for both image acquisition and data processing can produce similar results[13]. Techniques (including deconvolution) are applicable to single- and multiphoton confocal imaging with similar advantages, as long as light exposure is tolerated by the living preparation used. In the future, design improvements will further enhance the utility 4D live imaging. These include, primarily, hardware that enhances the speed of focusing and excitation/emission filter changing, and availability of even more sensitive video cameras.

Disclosures

The authors declare no competing financial interests.

Acknowledgements

This work was supported by the U.S. National Institutes of Health Grant NS-024572 (to R.S.W.).

References

1. Frigault, M. M., Lacoste, J., Swift, J. L., & Brown, C. M. Live-cell microscopy-tips and tools. *J. Cell Sci.* **122**(6), 753-767 (2009).
2. Tinevez, J.-Y., *et al.* A quantitative method for measuring phototoxicity of a live cell imaging microscope. *Meth. Enzymol.* **506,** 291-309 (2012).
3. Dunn, K.W., Kamocka, M.M., & McDonald, J. H. A practical guide to evaluating colocalization in biological microscopy. *Am. J. Physiol. Cell Physiol.* **300,** C723-C742 (2011).
4. Snapp, E. L., & Hegde, R. S. Rational design and evaluation of FRETexperiments to measure proteinproximities in cells. *Curr. Protoc. Cell Biol.* **17,** 17.9.1-17.9.20 (2006).
5. Stewart, R. S., Teng, H., & Wilkinson, R. S. "Late" macroendosomes and acidic endosomes in vertebrate motor nerve terminals. *J. Comp. Neurol.* **520,** 4275-4293 (2012).
6. Teng, H., Lin, M. Y., & Wilkinson, R. S. Macroendocytosis and endosome processing in snake motor boutons *J. Physiol.* **582.1,** 243-262 (2007).
7. McNally, J.G., Karpova, T., Cooper, J., & Conchello, J. A. Three-dimensional imaging by deconvolution microscopy. *Methods.* **19,** 373-385 (1999).
8. Swedlow, J. R., & Platani, M. Live cell imaging using wide-field microscopy and deconvolution. *Cell Struct. Funct.* **27,** 335-341 (2002).
9. Cromey, D. W. Digital images are data: and should be treated as such. In: *Cell imaging techniques: methods and protocols* (D. J. Taatjes and J. Roth, eds). **Methods Mol. Biol. 931**, 1-28 (2013).
10. Teng, H., & Wilkinson, R. S. Clathrin-mediated endocytosis near active zones in snake motor terminals. *J. Neurosci.* **20**(21), 7986-7993 (2000).
11. Teng, H., Cole, J. C., Roberts, R. L., & Wilkinson, R. S. Endocytic active zones: hot spots for endocytosis in vertebrate nerve terminals. *J. Neurosci.* **19**(12), 4855-4866 (1999).
12. Tan, T.T.T., Khaw, C., & Ng, M.M.L. Challenges and recent advances in live cell bioimaging. *Microscopy: Science, Technology, Applications and Education.* Mendez-Vilas, A., & Diaz, J. eds. 1495-1505 (2010).
13. Verbrugghe, K. J. C., & Chan, R. C. Imaging *C. elegans* embryos using an epifluorescent microscope and open source software. *J. Vis. Exp.* (49), e2625, doi:10.3791/2625 (2011).

